Brain-state- and cell-type-specific firing of hippocampal interneurons *in vivo*

Thomas Klausberger*, Peter J. Magill*, László F. Márton*, J. David B. Roberts*, Philip M. Cobden*, György Buzsáki† & Peter Somogyi*

** MRC Anatomical Neuropharmacology Unit, Department of Pharmacology, Oxford University, Mansfield Road, Oxford OX1 3TH, UK*
† Center for Molecular and Behavioral Neuroscience, Rutgers, The State University of New Jersey, Newark, New Jersey 07102, USA

Neural-network oscillations at distinct frequencies have been implicated in the encoding, consolidation and retrieval of information in the hippocampus. Some GABA (γ-aminobutyric acid)-containing interneurons fire phase-locked to theta oscillations (4–8 Hz) or to sharp-wave-associated ripple oscillations (120–200 Hz), which represent different behavioural states[1–6]. Interneurons also entrain pyramidal cells *in vitro*[7]. The large diversity of interneurons[8–10] poses the question of whether they have specific roles in shaping distinct network activities *in vivo*. Here we report that three distinct interneuron types—basket, axo-axonic and oriens–lacunosum-moleculare cells—visualized and defined by synaptic connectivity as well as by neurochemical markers, contribute differentially to theta and ripple oscillations in anaesthetized rats. The firing patterns of individual cells of the same class are remarkably stereotyped and provide unique signatures for each class. We conclude that the diversity of interneurons, innervating distinct domains of pyramidal cells[11], emerged to coordinate the activity of pyramidal cells in a temporally distinct and brain-state-dependent manner.

Network activity patterns of the hippocampus include theta oscillations (4–8 Hz), which are observed in the rat during exploration and rapid-eye-movement sleep[1,6], and sharp-wave-associated

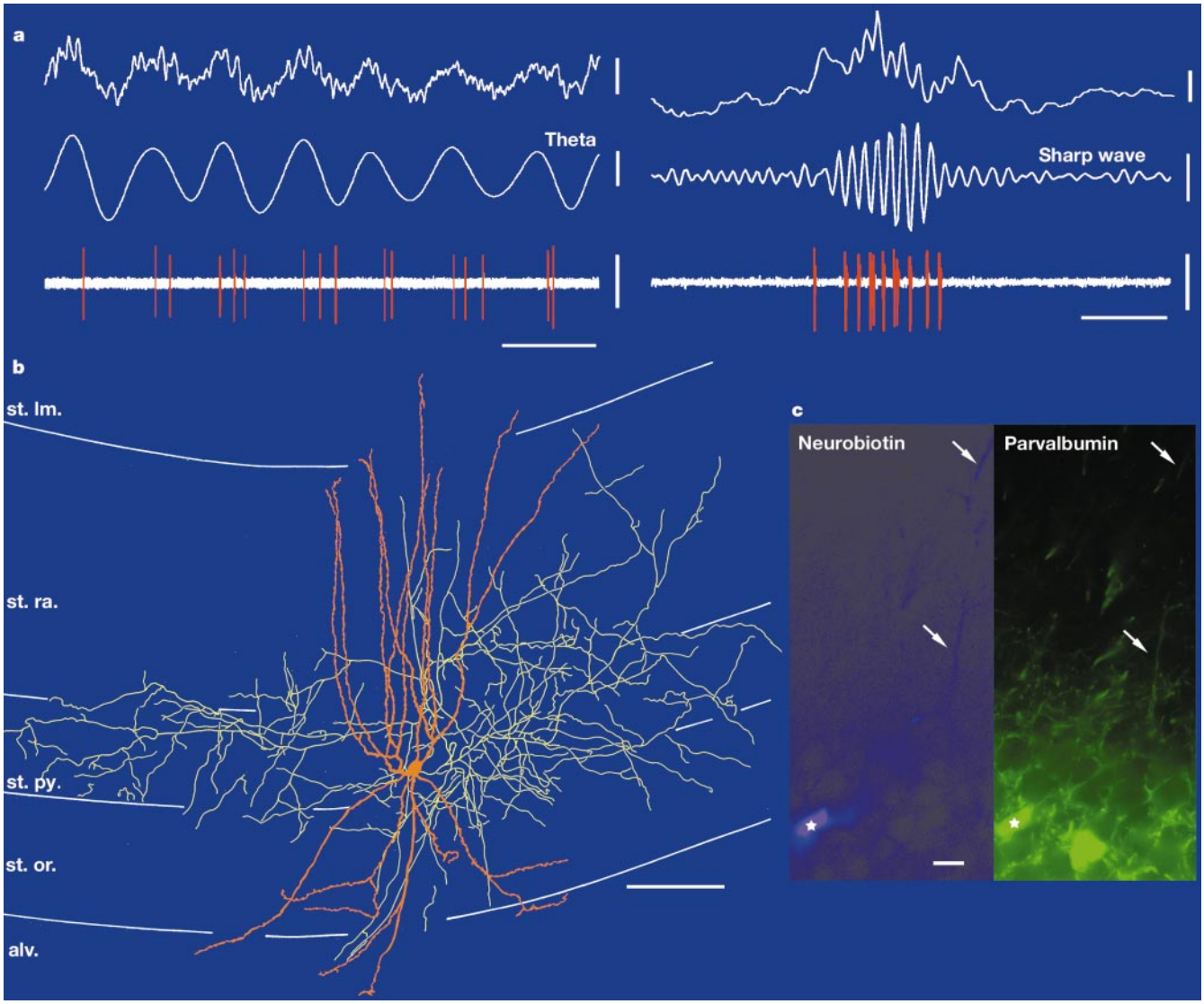

Figure 1 Firing patterns of a parvalbumin-positive basket cell (T44b) *in vivo*. **a**, The cell fired rhythmically on the descending phase of theta oscillations (filtered 3–6 Hz), and at high frequency at the troughs of sharp-wave-associated ripples (filtered 90–140 Hz). Scales: unit, 0.5 mV; unfiltered local field potential (LFP), 0.5 mV; theta, 0.3 mV, 300 ms; sharp wave, 0.2 mV, 50 ms. **b**, Reconstruction of the recorded and neurobiotin-labelled cell; soma and dendrites in red (complete). The axon in yellow, shown from only two sections of 65 μm thickness, contacted mainly pyramidal cell somata and proximal dendrites. **c**, The soma (star; partly seen) was cut during sectioning of the brain and is parvalbumin-immunopositive together with the dendrites (arrows) in immunofluorescence. alv., alveus; st. lm., stratum lacunosum-moleculare; st. or., stratum oriens; st. py., stratum pyramidale; st. ra., stratum radiatum. Scale bars: **b**, 100 μm; **c**, 20 μm.

ripples (120–200 Hz) that occur during slow-wave sleep, awake immobility and consumatory behaviours[3,5,12]. We recorded the spiking activity of GABA-releasing interneurons from the dorsal CA1 region of the hippocampus in anaesthetized rats during network oscillations. Under the combined urethane–ketamine anaesthesia used here, high-frequency ripples (mean ± s.d., 123 ± 11 Hz) occurred spontaneously, and theta oscillations (4.2 ± 0.3 Hz) occurred after foot-pinch or spontaneously, depending on the depth of anaesthesia. Importantly, systemic administration of atropine (75 mg kg^{-1}) did not abolish theta oscillations (4.0 ± 0.3 Hz) in five rats tested. The presence of atropine-resistant theta is similar to that observed in the behaving rat and different from rats deeply anaesthetized with urethane[13]. The application of the juxtacellular method[14] enabled us to label selectively the recorded neurons and to confirm their identity. Three distinct interneuron classes have been analysed by light and electron microscopy, as well as by immunocytochemical testing for neuropeptides, calcium-binding proteins and neurotransmitter receptors.

Parvalbumin-expressing basket cells ($n = 5$) fired preferentially on the descending phase of the extracellular theta oscillations recorded in the stratum pyramidale. They fired often with one or several spikes (Fig. 1a) per ripple episode, at 12° ± 69° (mean angle ± angular deviation) after the troughs of the ripple waves. The axon of basket cells was restricted mainly to the stratum pyramidale, or it also spread into neighbouring layers (Fig. 1b), but it predominantly contacted somata and proximal dendrites of pyramidal cells and other interneurons[11]. The somata of two basket cells were located in the stratum pyramidale; the other three somata were in stratum oriens, including one next to the alveus. No physiological difference was observed between cells that had different soma locations. All basket cells were immunopositive for

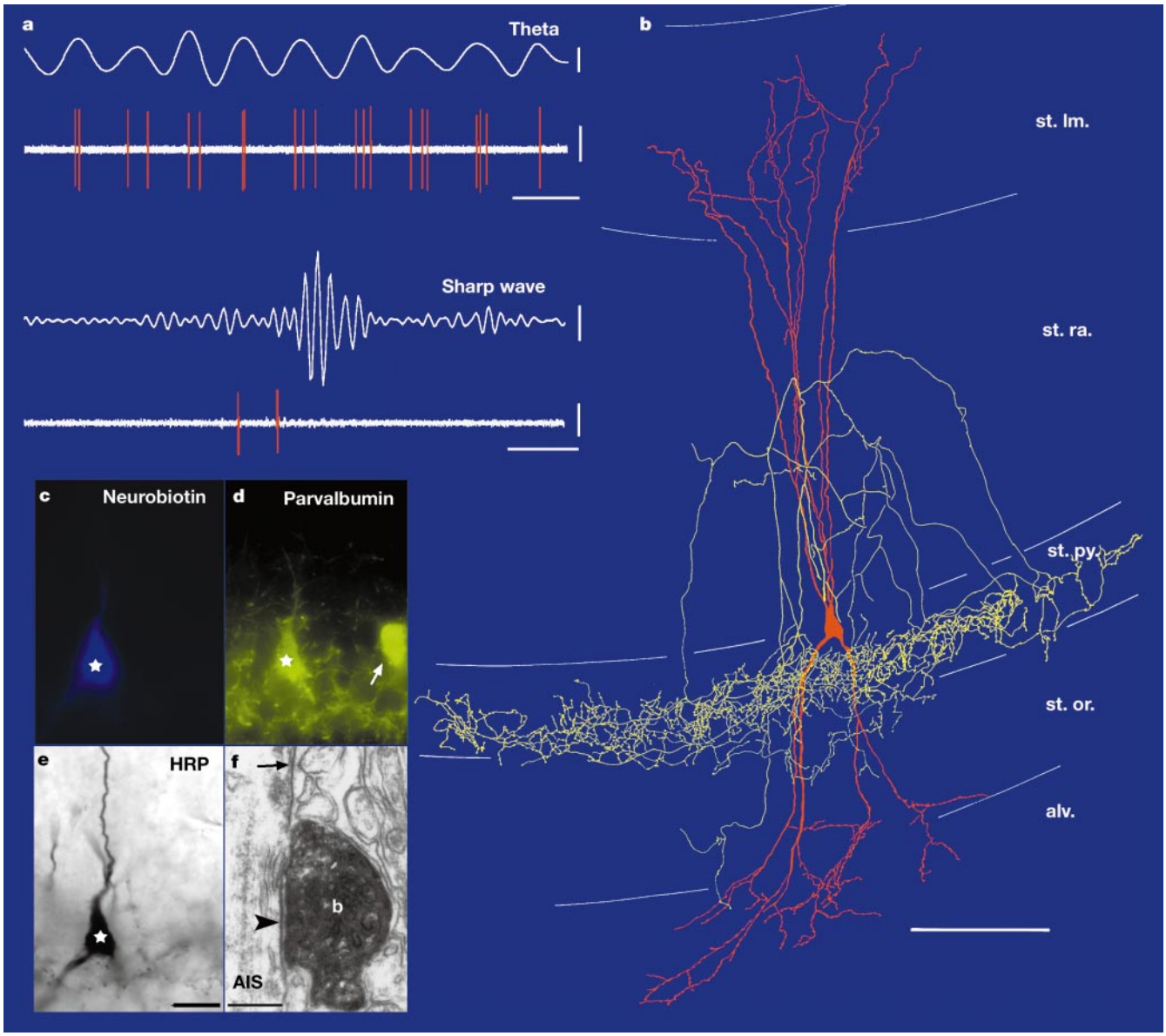

Figure 2 Firing patterns of a parvalbumin-positive axo-axonic cell (T76b) *in vivo*. **a**, The cell fired rhythmically just after the positive peak of theta oscillations, and at the beginning of a sharp-wave burst, but was silent subsequently. Scales: unit, 0.5 mV; theta, 0.2 mV, 300 ms; sharp wave, 0.1 mV, 50 ms. **b**, Reconstruction of the neurobiotin-labelled cell; soma and dendrites in red (complete); the axon (yellow) is restricted to the basal part of the stratum pyramidale and is shown from only one section of 65-μm thickness. **c**, **d**, Immunofluorescence of parvalbumin in the axo-axonic (star) and in an unrecorded cell (arrow). **e**, Micrograph of the labelled cell. **f**, Electron micrograph showing a bouton (b) making a synapse (arrowhead) with an axon initial segment (AIS) characterized by membrane undercoating (small arrow). Abbreviations as in Fig. 1. Scale bars: **b**, 100 μm, **c**–**e**, 20 μm; **f**, 0.2 μm.

parvalbumin (Fig. 1c), but were negative for the neuropeptide cholecystokinin (CCK).

Axo-axonic cells ($n = 2$) fired preferentially just after the peak of the theta cycles and discharged transiently at the beginning of sharp-wave-associated ripples (Fig. 2a). The somata of both cells were located in stratum pyramidale. In contrast to the basket cells, the dendrites of the axo-axonic cells branched extensively in stratum lacunosum-moleculare and in the alveus (Fig. 2b). Electron microscopic analysis confirmed the identity of these cells (Fig. 2f), as their postsynaptic targets were exclusively axon initial segments (13 synapses, cell T76b; eight synapses, cell T88a) of pyramidal cells[11]. Both axo-axonic cells were strongly immunopositive for parvalbumin (Fig. 2d); one of the cells was tested for CCK and was immunonegative (data not shown).

Oriens–lacunosum-moleculare (O-LM) cells ($n = 3$) fired rhythmically at the trough of theta cycles and were suppressed during ripple episodes (Fig. 3a). The somata of all three cells were located in the stratum oriens; one cell was at the border of the CA1 area and subiculum (Fig. 3b). They had mainly horizontally running dendrites. The main axons of these cells crossed stratum pyramidale and radiatum, and branched heavily in stratum lacunosum-moleculare, where their terminals are co-aligned with the entorhinal input[15–18]. All three O-LM cells were immunopositive for the metabotropic glutamate receptor mGluR1α and the neuropeptide somatostatin, and they were also weakly positive for parvalbumin (Fig. 3c). In addition, one of the cells was tested with an antibody against mGluR7a, and the soma and dendrites were selectively decorated with strongly immunopositive terminals (Fig. 3d).

To compare the firing patterns of different neurons quantitatively[5] (see also Supplementary Information), data from three different brain states were analysed: theta oscillation, sharp-wave/ripple epochs and non-theta/non-sharp-wave periods (Fig. 4a). The discharge frequency of pyramidal cells showed no significant difference (paired t-test, $P > 0.1$, $n = 6$) between theta and non-theta/non-sharp-wave periods. Interneurons, as a single group, increased their discharge frequency during theta oscillations (paired t-test, $P < 0.01$, $n = 10$). During ripples, both pyramidal cells and basket cells increased their discharge frequency (paired t-test, $P < 0.05$ and $P < 0.01$, respectively) in comparison to non-theta/non-sharp-wave periods. Axo-axonic cells showed no significant difference in discharge frequency (paired t-test, $P > 0.1$), and O-LM cells decreased their firing rates during sharp waves (paired t-test, $P < 0.05$).

An even more robust difference between interneuron classes emerged from the analysis of temporal structure during network oscillations (Fig. 4b). During theta oscillations, pyramidal cells fired at 20° ± 65°, parvalbumin basket cells at 271° ± 68°, axo-axonic cells at 185° ± 55°, and O-LM cells at 19° ± 57° (mean angle ± angular deviation). The phase preferences of the three interneuron classes during theta oscillations were all significantly different from each other (Watson–Williams test, $P < 0.01$). Notably, the interspike interval within theta cycles that had ≥2 spikes was different for the three cell types (Kruskal–Wallis test with post-hoc Dunn tests, $P < 0.01$). The interspike intervals were 45 ± 25 ms (mean ± s.d.), 20 ± 17 ms and 76 ± 19 ms for basket, axo-axonic and O-LM cells, respectively. This indicates that axo-axonic cells and basket cells discharge at gamma frequency within theta cycles, in contrast to O-LM cells. During sharp-wave-associated ripples, pyramidal cells and basket cells fired most frequently at the maximum amplitude of the ripple episode, resulting in a single, robust peak in the cross-correlogram (Fig. 4b). Surprisingly, both axo-axonic cells showed a different firing pattern; they increased their firing probability at the beginning of the sharp-wave episode, but were silent at the maximum amplitude and after the sharp wave. All O-LM cells were silent during sharp waves. The firing patterns of cells in the same class were remarkably similar, providing highly predictive signatures for each class. In addition, the firing patterns of the three classes of interneuron correspond to firing patterns of unidentified neurons in the behaving animal[5]. All parvalbumin-positive basket, axo-axonic and O-LM cells resemble 'single peak', 'biphasic' and

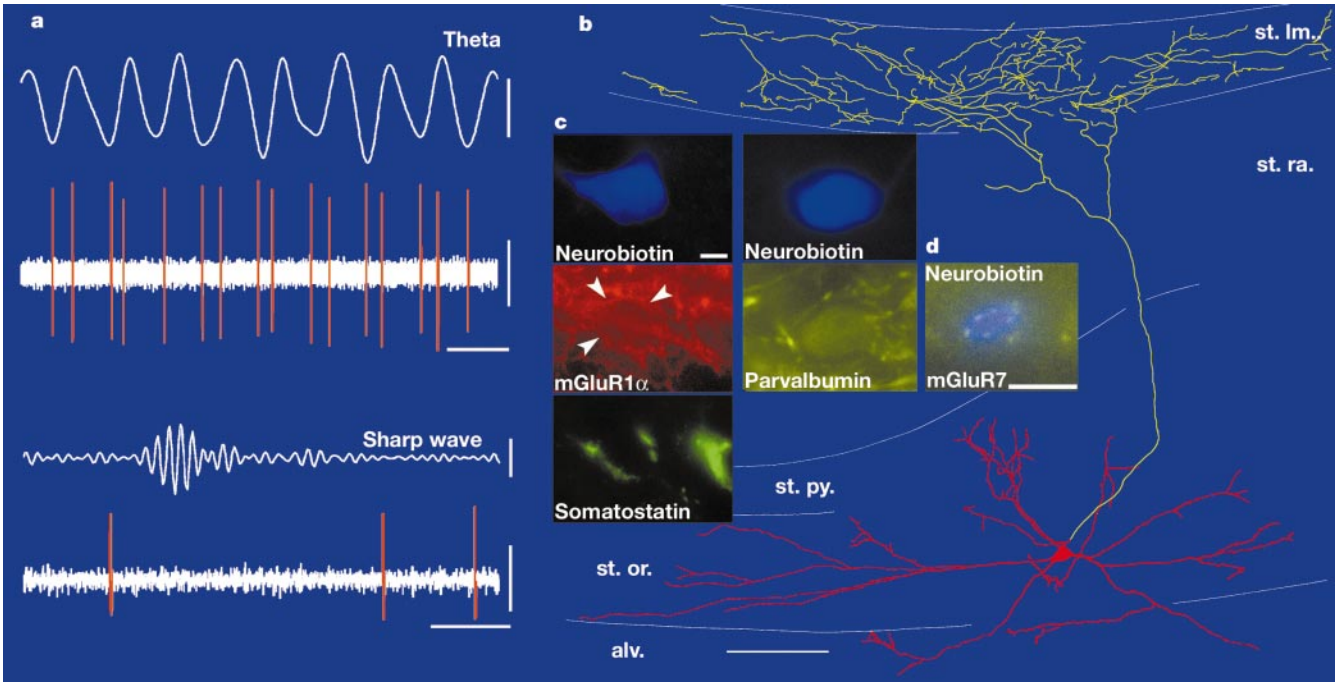

Figure 3 Firing patterns of an O-LM cell (T64a) *in vivo*. **a**, The cell fired rhythmically on the trough of theta oscillations, but was silent during sharp-wave-associated ripples. Scales: unit, 0.3 mV; theta, 0.2 mV, 300 ms; sharp wave, 0.05 mV, 50 ms. **b**, Reconstruction of the neurobiotin-filled oriens–lacunosum-moleculare (O-LM) cell. Soma and dendrites in red (complete); the axon restricted to str. lm. (yellow) is shown from only two sections of 65-μm thickness. **c**, The soma was cut into two sections; one shows somatostatin and metabotropic glutamate receptor mGluR1α immunoreactivity; the other shows parvalbumin immunoreactivity. **d**, The dendrite of another recorded O-LM cell (T93b) is decorated with highly mGluR7a-immunopositive terminals (yellow). Abbreviations as in Fig. 1. Scales: **b**, 100 μm; **c**, **d**, 5 μm.

'anti-sharp-wave' neurons, respectively (see Methods). One of the O-LM cells did not reach significance for anti-sharp-wave neurons, because only a small number of ripples ($n = 10$) could be recorded. Nevertheless, the data confirmed that O-LM cells are silent during sharp waves.

We have shown that three distinct classes of interneuron, as defined by their synaptic connectivity, contribute to different aspects of network oscillations *in vivo*. Therefore, it seems that a large diversity of GABA interneurons evolved to control pyramidal cells in a temporally distinct and brain-state-dependent manner. During theta activity, CA1 place cells[1] are activated primarily by the perforant path[19,20]. The O-LM cells, whose axons are co-aligned with the perforant path input, fire coincidentally with the strongest hyperpolarization in the distal dendrites of pyramidal cells[6]. Therefore, O-LM cells might phase-modulate excitatory input from the perforant path[21] and/or provide rhythmic hyperpolarization that could de-inactivate voltage-sensitive ion channels and facilitate somatodentritic back-propagation of the action potentials[22] and burst discharge[23] in active place cells. Axo-axonic cells and basket cells have high discharge probabilities on the descending phase of the theta cycle at times when the discharge probability of pyramidal cells is lowest and gamma power is highest[2,6,24–26]. Such cycle-phase arrangement can facilitate the rhythmic entrainment of pyramidal cell discharge[7]. During slow-wave sleep, the main driving source to CA1 pyramidal neurons is the sharp-wave-associated discharge of the CA3 pyramids[5]. Transient suppression of O-LM cell activity during sharp waves may allow action potentials in pyramidal cells to back-propagate to the most distal dendrites[27,28] and facilitate long-term potentiation of those entorhinal input synapses that are coincidentally active during sharp waves. Basket cells (parvalbumin-positive) fire at high frequency and phase-locked to ripple oscillation, and can therefore provide an inhibitory temporal structure for large populations of pyramidal cells[3,5]. By contrast, axo-axonic cells, which make inhibitory synapses at the site of action potential generation, only fire at the beginning of the sharp wave. Such a coordination of distinct inputs could time-lock the activity of thousands of pyramidal cells to fire together, exactly at the maximum amplitude of ripple episodes.

Different classes of interneuron innervate distinct domains of pyramidal cells and exhibit specific firing patterns during behaviourally relevant oscillations. Therefore, they probably evolved to temporally coordinate input–output transformation in the hippocampal pyramidal cells, and to govern the formation and retrieval of cell assemblies during hippocampus-dependent behaviour. □

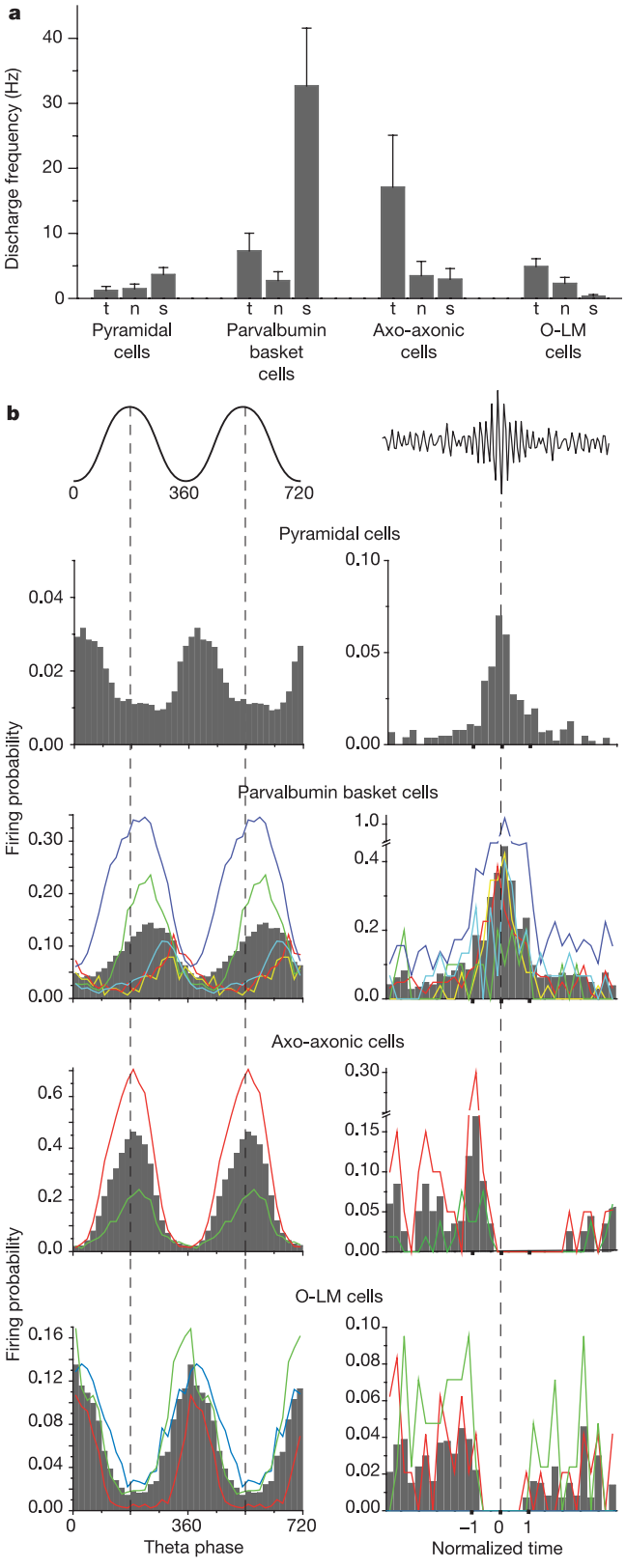

◀ **Figure 4** Distinct interneuron classes generate different firing patterns during theta and ripple oscillations *in vivo*. **a**, Discharge frequency (mean ± s.e.m.) of pyramidal cells, parvalbumin-positive basket cells, axo-axonic cells and O-LM cells during theta (t), non-theta/non-sharp-wave (n) and sharp-wave-associated ripples (s). **b**, The mean firing probabilities of different cell types are shown as grey columns, firing probabilities of each interneuron as coloured lines. For clarity, two theta cycles are shown; 0° and 360° mark the trough of the theta cycles recorded extracellularly in the stratum pyramidale (left column). The start, maximum amplitude and end of the normalized sharp-wave episodes are marked as −1, 0 and 1, respectively (right column). Note that the phase relationships of neurons to the network patterns are similar within the same class, despite variation in discharge probability of individual cells.

Methods

Electrophysiological recordings

Rats were treated in accordance with the Animals (Scientific Procedures) Act, 1986 (UK) and associated procedures. Fifty-two male Sprague–Dawley rats (250–350 g) were anaesthetized with 1.25 mg kg^{-1} urethane, plus supplemental doses of ketamine and xylazine (20 and 2 mg kg^{-1}, respectively) as needed, and body temperature was retained with a heating pad. Neuronal activity in the hippocampus was recorded extracellularly with a glass electrode (18–25 MΩ) filled with 1.5% neurobiotin in 0.5 M NaCl, and the local field potential (LFP) was recorded with a stationary second electrode in the hippocampal CA1 pyramidal cell layer. Single-unit activity (sampling rate 20 kHz) and LFP (sampling rate 800 Hz) were filtered online at 0.8–5 kHz and 0.5–200 Hz, respectively. After the collection of a sufficient number of spikes, the electrode was advanced towards the cell, which was then labelled juxtacellularly with neurobiotin by applying positive current steps[14]. The shape and amplitude of spikes were monitored during recording, advancing the electrode and labelling to ensure that recorded spikes originated from a single neuron only, and that the recorded cell was labelled. Recordings from nine out of ten putative interneurons resulted in a single labelled interneuron following histological

processing. In one case, spikes from a putative interneuron and a putative pyramidal cell were recorded simultaneously and, after labelling, a parvalbumin-positive basket cell and a pyramidal cell were recovered. The interneuron was more strongly modulated by the current steps and was also more strongly labelled than the pyramidal cell.

Anatomical and immunohistochemical visualization

The rats were perfused with fixative 4 h after labelling. Immunofluorescence and peroxidase reactions for light microscopy and electron microscopy were performed as described previously[18,29]. Antibodies against parvalbumin, CCK, somatostatin and mGluR7a were gifts from K. Baimbridge, A. Varro, A. Buchan and R. Shigemoto, respectively; antibodies against mGluR1 were obtained from DiaSorin. The specificity of these antibodies is discussed elsewhere[29].

Data analysis

Theta epochs were detected by calculating the theta (3–6 Hz) to delta (2–3 Hz) frequency power ratio in 2-s windows of the LFP[5]. A ratio greater than four in at least three consecutive windows marked theta episodes, and a ratio less than two in at least three consecutive windows indicated epochs that are called non-theta/non-sharp-wave periods, which lacked field ripples. Non-theta/non-sharp-wave periods contained oscillations of 1 Hz and/or 2–3 Hz, but were not further analysed in this study, owing to the larger variability in cell activity. To determine the phase relationship between single-cell and theta activity, the troughs of the theta oscillations were detected in the filtered signal (3–6 Hz). Each spike was assigned to a given phase (bin size 20°) between the troughs (0° and 360°) and all theta cycles were superimposed[5]. Theta phase was analysed using circular statistics[30].

The LFP was filtered at 90–140 Hz for the detection of sharp-wave-associated ripples and the power (r.m.s. amplitude) of the filtered signal was calculated in 10-ms windows[5]. The threshold for ripple detection was set to 5 s.d. above the mean power. The beginning and the end of the sharp wave were set where the power crossed 1 s.d. above the mean power. The maximum amplitude of the oscillation was detected by a peak-finding algorithm. To evaluate the firing pattern of a single neuron during sharp waves, ripple episodes were normalized. Because sharp waves are often not symmetrical, the periods between the beginning and the ripple maximum, and the ripple maximum and the end of the sharp-wave episodes were each divided into four bins, and spikes were sorted into bins. To test whether potential correlations of firing patterns with sharp waves arose by chance, for each cell the exact number and duration of observed sharp-wave windows were randomly shuffled over the period of non-theta/non-sharp-wave epoch, and the spikes detected in the windows were binned. A neuron was considered to be a 'single peak' cell if the number of spikes in six bins surrounding the ripple maximum was higher in the observed sharp-wave correlogram than the mean + 2 s.d. from 100 shuffled correlograms. For anti-sharp-wave cells the number of spikes in six bins surrounding the ripple maximum was lower in the observed sharp wave correlogram than the mean − 2 s.d. from 100 shuffled correlograms. For biphasic neurons, the number of spikes in four bins surrounding the beginning of the sharp wave was higher in the observed sharp-wave correlogram than the mean + 1 s.d. from 100 shuffled correlograms, and the number of spikes in ten consecutive bins, starting from the fourth bin of the sharp wave, was lower in the observed sharp waves than the mean − 2 s.d. of the respective bins from 100 shuffled correlograms. The discharge frequency of single cells during three different brain states (theta, sharp-wave and non-theta/non-sharp-wave) was calculated by dividing the number of spikes with the summed duration of the respective brain state.

Received 15 October; accepted 29 November 2002; doi:10.1038/nature01374.

1. O'Keefe, J. & Nadel, L. *The Hippocampus as a Cognitive Map* (Clarendon, Oxford, UK, 1978).
2. Fox, S. E. Membrane potential and impedance changes in hippocampal pyramidal cells during theta rhythm. *Exp. Brain Res.* **77,** 283–294 (1989).
3. Ylinen, A. *et al.* Sharp wave-associated high-frequency oscillation (200 Hz) in the intact hippocampus: Network and intracellular mechanisms. *J. Neurosci.* **15,** 30–46 (1995).
4. Ylinen, A. *et al.* Intracellular correlates of hippocampal theta rhythm in identified pyramidal cells, granule cells, and basket cells. *Hippocampus* **5,** 78–90 (1995).
5. Csicsvari, J., Hirase, H., Czurko, A., Mamiya, A. & Buzsáki, G. Oscillatory coupling of hippocampal pyramidal cells and interneurons in the behaving rat. *J. Neurosci.* **19,** 274–287 (1999).
6. Buzsáki, G. Theta oscillations in the hippocampus. *Neuron* **33,** 325–340 (2002).
7. Cobb, S. R., Buhl, E. H., Halasy, K., Paulsen, O. & Somogyi, P. Synchronization of neuronal activity in hippocampus by individual GABAergic interneurons. *Nature* **378,** 75–78 (1995).
8. Freund, T. F. & Buzsáki, G. Interneurons of the hippocampus. *Hippocampus* **6,** 347–470 (1996).
9. Fricker, D. & Miles, R. Interneurons, spike timing, and perception. *Neuron* **32,** 771–774 (2001).
10. McBain, C. J. & Fisahn, A. Interneurons unbound. *Nature Rev. Neurosci.* **2,** 11–23 (2001).
11. Buhl, E. H., Halasy, K. & Somogyi, P. Diverse sources of hippocampal unitary inhibitory postsynaptic potentials and the number of synaptic release sites. *Nature* **368,** 823–828 (1994).
12. Traub, R. D. *et al.* Axonal gap junctions between principal neurons: A novel source of network oscillations, and perhaps epileptogenesis. *Rev. Neurosci.* **13,** 1–30 (2002).
13. Vanderwolf, C. H. Cerebral activity and behavior: Control by central cholinergic and serotonergic systems. *Int. Rev. Neurobiol.* **30,** 225–340 (1988).
14. Pinault, D. A novel single-cell staining procedure performed *in vivo* under electrophysiological control: Morpho-functional features of juxtacellularly labeled thalamic cells and other central neurons with biocytin or neurobiotin. *J. Neurosci. Methods* **65,** 113–136 (1996).
15. McBain, C. J., DiChiara, T. J. & Kauer, J. A. Activation of metabotropic glutamate receptors differentially affects two classes of hippocampal interneurons and potentiates excitatory synaptic transmission. *J. Neurosci.* **14,** 4433–4445 (1994).
16. Sik, A., Penttonen, M., Ylinen, A. & Buzsáki, G. Hippocampal CA1 interneurons: An *in vivo* intracellular labeling study. *J. Neurosci.* **15,** 6651–6665 (1995).
17. Ali, A. B. & Thomson, A. M. Facilitating pyramid to horizontal oriens–alveus interneurone inputs: Dual intracellular recordings in slices of rat hippocampus. *J. Physiol. (Lond.)* **507,** 185–199 (1998).
18. Maccaferri, G., Roberts, J. D. B., Szucs, P., Cottingham, C. A. & Somogyi, P. Cell surface domain specific postsynaptic currents evoked by identified GABAergic neurones in rat hippocampus *in vitro*. *J. Physiol. (Lond.)* **524,** 91–116 (2000).
19. Nakazawa, K. *et al.* Requirement for hippocampal CA3 NMDA receptors in associative memory recall. *Science* **297,** 211–218 (2002).
20. Brun, V. H. *et al.* Place cells and place recognition maintained by direct entorhinal–hippocampal circuitry. *Science* **296,** 2243–2246 (2002).
21. Gillies, M. J. *et al.* A model of atropine-resistant theta oscillations in rat hippocampal area CA1. *J. Physiol. (Lond.)* **543,** 779–793 (2002).
22. Spruston, N., Schiller, Y., Stuart, G. & Sakmann, B. Activity-dependent action potential invasion and calcium influx into hippocampal CA1 dendrites. *Science* **268,** 297–300 (1995).
23. Harris, K. D., Hirase, H., Leinekugel, X., Henze, D. A. & Buzsáki, G. Temporal interaction between single spikes and complex spike bursts in hippocampal pyramidal cells. *Neuron* **32,** 141–149 (2001).
24. Skaggs, W. E., McNaughton, B. L., Wilson, M. A. & Barnes, C. A. Theta phase precession in hippocampal neuronal populations and the compression of temporal sequences. *Hippocampus* **6,** 149–172 (1996).
25. Mehta, M. R., Lee, A. K. & Wilson, M. A. Role of experience and oscillations in transforming a rate code into a temporal code. *Nature* **417,** 741–746 (2002).
26. Harris, K. D. *et al.* Spike train dynamics predicts theta-related phase precession in hippocampal pyramidal cells. *Nature* **417,** 738–741 (2002).
27. Katona, I., Acsady, L. & Freund, T. F. Postsynaptic targets of somatostatin-immunoreactive interneurons in the rat hippocampus. *Neuroscience* **88,** 37–55 (1999).
28. Magee, J. C. & Johnston, D. A synaptically controlled, associative signal for Hebbian plasticity in hippocampal neurons. *Science* **275,** 209–213 (1997).
29. Losonczy, A., Zhang, L., Shigemoto, R., Somogyi, P. & Nusser, Z. Cell type dependence and variability in the short-term plasticity of EPSCs in identified mouse hippocampal interneurones. *J. Physiol. (Lond.)* **542,** 193–210 (2002).
30. Zar, J. H. *Biostatistical Analysis* (Prentice Hall, New Jersey, 1999).

Supplementary Information accompanies the paper on *Nature*'s website (**http://www.nature.com/nature**).

Acknowledgements We thank G. Horseman and S. Gray from Cambridge Electronic Design, and P. Jays and L. Norman for technical assistance. We thank Z. Nusser, G. Tamas and J. Csicsvari for critically reading an earlier version of the manuscript, and Y. Dalezios for help with the statistics. T.K. was supported by an Erwin Schroedinger Fellowship from the Austrian Science Fund during part of this study; G.B. was supported by the National Institutes of Health.

Competing interests statement The authors declare that they have no competing financial interests.

Correspondence and requests for materials should be addressed to T.K. (e-mail: thomas.klausberger@pharm.ox.ac.uk).

Yeast genome duplication was followed by asynchronous differentiation of duplicated genes

Rikke B. Langkjær*, Paul F. Cliften†, Mark Johnston† & Jure Piškur*

** BioCentrum-DTU, Technical University of Denmark, Building 301, DK-2800 Lyngby, Denmark*

† Department of Genetics and Genome Sequencing Center, Washington University School of Medicine, St. Louis, Missouri 63110, USA

Gene redundancy has been observed in yeast, plant and human genomes, and is thought to be a consequence of whole-genome duplications[1–3]. Baker's yeast, *Saccharomyces cerevisiae*, contains several hundred duplicated genes[1]. Duplication(s) could have occurred before or after a given speciation. To understand the evolution of the yeast genome, we analysed orthologues of some of these genes in several related yeast species. On the basis of the inferred phylogeny of each set of genes, we were able to deduce whether the gene duplicated and/or specialized before or after the divergence of two yeast lineages. Here we show that the gene duplications might have occurred as a single event, and that it probably took place before the *Saccharomyces* and *Kluyveromyces* lineages diverged from each other. Further evolution of each duplicated gene pair—such as specialization or differentiation of

Supplementary Table

Firing patterns of single interneurons

Cell	Cell type	Discharge Frequency [Hz] t	n	s	Mean theta angle±angular deviation	Firing pattern during ripples	Median No spikes/ripple episode*
T44b	basket	3.4	0.4	14.7	317°±65°	single peak	2
T68a	basket	8.2	3.1	25.6	233°±57°	single peak	1
T75aa	basket	17.6	7.9	64.9	200°±66°	single peak	4
T75ab	basket	3.8	1.3	20.6	319°±62°	single peak	1
T80b	basket	3.5	1.0	37.6	279°±60°	single peak	1
T76b	axo-axonic	9.1	1.3	1.3	192°±55°	biphasic	1
T88a	axo-axonic	25.1	5.7	4.6	178°±55°	biphasic	1
T64a	O-LM	6.1	1.9	0.4	24°±65°	anti-sharp wave	0
T69e	O-LM	2.5	0.9	0.0	27°±45°	-	0
T93b	O-LM	6.1	4.1	0.3	2°±58°	anti-sharp wave	0

t, n, s indicate theta, non-theta/non-sharpwave, and sharp wave episodes, respectively.
*The number of ripple events used for these analyses varied from 10 to 62 (basket cells), 20 to 57 (axo-axonic) and 10 to 48 (O-LM cells).